Environ Monit Assess (2016) 188:285
DOI 10.1007/s10661-016-5293-4

Photosynthetic pigment laser-induced fluorescence indicators for the detection of changes associated with trace element stress in the diatom model species *Phaeodactylum tricornutum*

Maria Teresa Cabrita · Carla Gameiro · Andrei B. Utkin · Bernardo Duarte · Isabel Caçador · Paulo Cartaxana

Received: 21 August 2015 / Accepted: 5 April 2016

Abstract This work reports changes on cell number, growth rate, trace element content, chlorophyll *a* (Chl *a*) and carotenoid concentrations, and laser-induced fluorescence (LIF) spectra of *Phaeodactylum tricornutum* exposed to Co, Ni, Cu, Zn, Cd, Hg, Pb, and a mixture of all elements combined (Mix). The total levels of trace elements associated with the cells were significantly higher in the exposed than in control ones. Concomitantly, specific cell growth was significantly lower in exposed *P. tricornutum*, suggesting that trace elements affected the microalgae physiology. The LIF emission spectra showed two typical emission bands in red (683–698 nm) and far-red (725–730 nm) regions. Deviations in LIF spectra and changes in F685/F735 ratio were investigated as indicators of trace element-induced changes. Fluorescence intensity emitted by exposed microalgae decreased in far-red region when compared to control cells, suggesting Chl *a* damage and impairment of pigment biosynthesis pathways by trace elements, confirmed by Chl *a* and carotenoid concentration decrease. Significant increase in F685/F735 ratio was detected for all elements except Zn and more accentuated for Co, Hg, and Mix. Significant deviations in wavelength emission maxima in red region were also more significant (between 8 and 13 nm) for Co, Hg, and Mix. Growth changes agreed with deviations in LIF spectra and F685/F735 ratio, supporting their applicability as indicators. This study clearly shows F685/F735 ratio and the deviations in wavelength emission maxima as adequate trace element stress indicators and *P. tricornutum* as a promising biomonitor model species. LIF-based techniques can be used as time-saving, highly sensitive, and effective alternative tool for the detection of trace element stress, with potential for remote sensing and trace element contamination screening in marine coastal areas.

Keywords Laser-induced fluorescence indicators · LIF · *Phaeodactylum tricornutum* · Trace element stress detection and monitoring · Marine coastal areas

M. T. Cabrita (✉)
Instituto Português do Mar e da Atmosfera (IPMA), Av. de Brasília, 1449-006 Lisbon, Portugal
e-mail: maria.teresa.cabrita@gmail.com

C. Gameiro · B. Duarte · I. Caçador
Centro de Ciências do Mar e Ambiente (MARE), Faculdade de Ciências da Universidade de Lisboa, Campo Grande, 1749-016 Lisbon, Portugal

A. B. Utkin
INOV-INESC, Rua Alves Redol 9, 1000-029 Lisboa, Portugal

A. B. Utkin
ICEMS, IST, Universidade Técnica de Lisboa, Av. Rovisco Pais 1, 1049-001 Lisbon, Portugal

P. Cartaxana
Marine Biological Section, Department of Biology, University of Copenhagen, Strandpromenaden 5, 3000 Helsingør, Denmark

Introduction

Fossil fuel combustion, industrial activity, and fertilizer use over the last decades have been responsible for

Published online: 13 April 2016

permanent trace element sediment contamination of urbanized estuarine and coastal areas (Doney 2010). Several elements such as Co, Ni, Cu, Zn, Cd, Hg, and Pb can be transferred from contaminated sediments into the water column in elevated concentrations, due to human activities, such as dredging, harbor or industrial trace element contaminated waste disposal activities (Eggleton and Thomas 2004). This trace element mobilization has deleterious effects in the ecosystems due to the persistent toxicity of several elements (Pan and Wang 2012), and because trace elements are transferred and biomagnified in marine food webs (Jakimska et al. 2011). The search for effective and reliable indicators for the detection of trace elements stress in these coastal systems is crucial due to the scale of this problem and the need for more effective regulation (Rogers and Greenaway 2005).

Phytoplankton constitutes the base of those marine webs, efficiently scavenging metals (González-Dávila 1995) and rapidly responding to changes on metal availability in the environment (Sunda and Huntsman 1998; Cabrita et al. 2014). Despite their varying degree of trace element tolerance, it has been shown that many phytoplankton species are highly sensitive to trace elements even in very low concentrations (Reed and Gadd 1989; Tortell and Price 1996). Once incorporated into phytoplankton cells, trace elements may cause disturbance of cell membrane permeability, reduction of photosynthetic electron transport and carbon fixation, degradation and biosynthesis inhibition of photosynthetic pigments, inhibition of enzyme reactions or protein synthesis, among other cellular functions (De Filippis and Pallaghy 1994; Sunda and Huntsman 1998; Küpper et al. 2002). Inevitably, these alterations have clear repercussions on phytoplankton cell growth (Thomas et al. 1980; Brand et al. 1986) and photosynthetic performance (Cid et al. 1995). Responses of phytoplankton to trace elements at the photosynthetic level may thus be potentially used for element contamination screening in marine ecosystems.

Chlorophyll *a* (Chl *a*) fluorescence is a sensitive indicator of the status of photochemical reactions (Buschmann 2007). In vivo Chl *a* fluorescence spectra of plants typically include two maxima, one in the red (685 to 690 nm) and one in the far-red (710 to 740 nm) regions, which are primarily dependent on the concentration of Chl *a* (Buschmann 2007). Most of this emission is linked to the pigment–protein complex photosystem II (PS II)-associated Chl *a* (Govindjee 1995), with the red band arising from the main electronic transitions, and the far-red band resulting from vibrational sublevels whose relative intensities are increased in vivo through self-absorption (Franck et al. 2002). Additionally, some fluorescence of the photosystem I (PS I), which is highest around 730 nm, also contributes to the fluorescence emitted at the far-red band (Govindjee 1995; Pfündel 1998). Alterations in the fluorescence intensity of Chl *a* indicate variations in Chl *a* concentration and have been pointed as one of the earliest indicators of physiological status in microalgae and other plants (Baker 2008). Therefore, interest in the practical application of Chl *a* fluorescence as a rapid and sensitive bioindicator of plant stress in response to different contaminants, including trace elements, has been growing in recent years (Kumar et al. 2014). Previous studies showed the red to far-red fluorescence ratio (F685/F735) as a promising indicator of different types of stress in plants (Lichtenthaler and Rinderle 1988; Schuerger et al. 2003; Buschmann 2007). However, the F685/F735 and other suitable Chl *a* fluorescence-based indicators need to be tested and identified for trace element stress detection and monitoring, taking into account the combination of trace elements, and their concentrations commonly found in contaminated marine coastal areas.

Among the various fluorescence techniques, laser-induced fluorescence (LIF) technique is a powerful non-destructive tool to determine the total amount of Chl *a* fluorescence resulting from a very small fraction (only 1 or 2 %) of total absorbed light. The high sensitivity and resolution of LIF has been shown to be well-suited for reliable estimation of plant Chl *a* concentrations and photosynthetic efficiency changes due to various plant environmental stressors (Dahn et al. 1992; D'Ambrosio et al. 1992; Subhash and Mohanan 1997; Apostol et al. 2003; Lavrov et al. 2012), including trace elements (Schuerger et al. 2003; Mishra and Gopal 2005; Maurya and Gopal 2008), and therefore has potential as an alternative tool for detecting signs of trace element stress in phytoplankton. This technique has been used in controlled laboratory conditions and in the field, with promising application to remote assessments.

The present work investigates effective and reliable Chl *a* fluorescence-based indicators for the detection of trace element stress in coastal systems, using the diatom species *Phaeodactylum tricornutum*. Here, we hypothesize that deviations in the peak center of Chl *a* fluorescence bands of LIF emission spectra, in addition to the F685/F735 ratio, may be such indicators, and that

P. tricornutum may be a promising biomonitor model species, and LIF a reliable, accurate and highly sensitive alternative tool for the detection of trace element stress in marine ecosystems. This study examines changes in Chl *a* fluorescence spectra of *P. tricornutum* exposed to different trace elements (Co, Ni, Cu, Zn, Cd, Hg, Pb, and mixture of all trace elements (Mix)), and possible consequences to Chl *a* content and photosynthetic performance. The species *P. tricornutum* is a cosmopolitan neritic diatom, tolerant to a wide range of temperature, salinity, and eutrophic conditions, which rapidly responds to trace element changes in the environment (Cabrita et al. 2014). This species was selected because it is representative of diatoms that recurrently dominate the phytoplankton communities in estuarine and coastal waters. To our knowledge, this is the first study to employ LIF to identify Chl *a* fluorescence-based indicators using a phytoplankton species exposed to a wide range of trace elements, simulating element combination and concentrations previously found in contaminated coastal areas.

Materials and methods

Trace element exposure experiments

Cells of the diatom *P. tricornutum* Bohlin (Bacillariophyceae), obtained from axenic cultures, were grown in f/2 medium (Guillard and Ryther 1962) at temperature-controlled conditions (18 ± 1 °C), constant aeration, and under a 14-h light/10-h dark cycle provided by a cool–white fluorescent light source (80 μmol photons m^{-2} s^{-1}). For the trace element exposure treatments, the cells collected during the exponential phase (4 days after inoculation) were concentrated by centrifuging (10 min at 2054×*g*), washed to remove complexing agents, metals, and excess nutrients from the f/2 media prior to the beginning of the experiments. Cells were subsequently resuspended in autoclaved seawater. Then, nutrients ($NaNO_3$, $NaH_2PO_4{\cdot}H_2O$, and $Na_2SiO_3{\cdot}9H_2O$) and vitamins were added to the seawater, as performed in previous similar incubation experiments (Cabrita et al. 2014), because in cell culture experiments, there is no renewal of seawater during the incubation period, as occurs in the natural environment, and seawater natural levels of nutrients do not support *P. tricornutum* culture growth during incubations lasting 4 days, as nutrients are rapidly consumed by the cells. That is the reason for adding $NaNO_3$, $NaH_2PO_4{\cdot}H_2O$, and $Na_2SiO_3{\cdot}9H_2O$ and vitamins to the clean seawater. Only this way, cells were at optimal growth rate and the potential decrease in growth and other changes associated with the enhancement of trace elements in the medium could be clearly evaluated. The trace elements Co ($CoCl_2{\cdot}6H_2O$), Ni ($NiCl_2$), Cu ($CuSO_4{\cdot}5H_2O$), Zn ($ZnSO_4{\cdot}7H_2O$), Cd ($CdCl_2$), Hg ($HgCl_2$), and Pb ($Pb(NO_3)_2$) were added to obtain final nominal elemental concentrations of 2.0, 2.0, 3.0, 14, 0.05, 0.1, and 0.2 μg L^{-1}, respectively, reproducing trace elements and concentrations previously found in contaminated coastal areas (Cotté-Krieff et al. 2000; Cabrita et al. 2014). Cells were also grown in a Mix and in the same individual concentrations, also commonly observed in contaminated coastal areas, thus allowing assessing the combined trace element effect. Relatively low initial cell density (4×10^{-5} cell mL^{-1}) was used in these experiments, following the Organization for Economic Cooperation and Development (OECD) guidelines for algae bioassays (OECD 2002) and the therein recommended initial cell density for microalgae cells with similar size to *P. tricornutum*, and also to better reflect cell concentrations found in marine coastal areas. All the exposure experiments were carried out in 250-mL glass Erlenmeyer flasks.

In parallel, the actual dissolved trace element concentrations at the beginning of the experiments were determined in 2-L replicates of the nonexposed and trace element-exposed cultures, using diffusive gradient in thin-films (DGT), as described in Cabrita et al. (2014). Chelex-100 resins and diffusive gels (type APA, 0.8-mm thickness, open pore) (Zhang and Davison 1999) were purchased from DGT Research (Lancaster, UK, http://www.dgtresearch.com). One DGT was deployed per flask with the same trace element levels of the nonexposed and exposed culture flasks, but with no addition of cells. The DGTs were suspended with a nylon thread inside each flask, at the same temperature- and light-controlled conditions used for the cell incubation experiments, and under similar constant aeration which produced the water flow across the face of the membranes necessary for the accurate determination of trace elements in the water at the beginning of the exposure experiments. After a 48-h period, the DGTs were carefully removed and resins were immersed in 5 mL of 1 M HNO_3. Element concentration were directly quantified in resin eluates by an inductively coupled plasma mass spectrometer (ICP-

MS) (Thermo Elemental, X-Series), equipped with a Peltier impact bead spray chamber and a concentric Meinhard nebulizer. All eluates were analyzed with reagent blanks to control eventual contaminations during the analytical procedure and with an international standard of river water (SLRS-5, from the National Research Council of Canada) to control the accuracy of the procedure. The eluate concentration was converted into the mass of trace element accumulated on the resin using an elution factor with a yield value of 0.8 (Zhang and Davison 1995) and a resin gel volume of 0.15 mL. The DGT-measured trace element concentrations (C_{DGT}) were calculated according to the following equation (Davison and Zhang 1994):

$$C_{DGT} = (M\Delta g) \Big/ (tAD) \quad (1)$$

where M is the mass of trace element accumulated on the resin during the emersion time (t), Δg is the diffusive gel thickness (0.08 cm), A is the exposure area (3.14 cm^2), and D is the diffusion coefficient of the trace element in the gel at 18 °C, as provided by DGT Research (Lancaster, UK, http://www.dgtresearch.com).

To detect trace element stress, nonexposed and trace element-exposed cell cultures were maintained for 4 days, under the same growth conditions used for the axenic cultures. Different culture sample volumes were analyzed after 2-day (20 mL) and 4-day (10 mL) incubations. All materials used were cleaned with HNO_3 (20 %) for 2 days and rinsed thoroughly with Milli-Q water (18.2 MΩ cm) to avoid trace element contamination. Culture manipulations were performed in a laminar air flow chamber.

Sample analysis

Samples of *P. tricornutum* of both control and trace element exposure experiments were rapidly filtered and retained in Whatman™ high efficiency Grade GF/F glass fiber filters, prior to LIF analysis. Immediately after LIF analysis, the filters were frozen at −20 °C, for Chl *a* and carotenoid quantification. Chl *a* and carotenoids were determined spectrophotometrically, according to Strickland and Parsons (1968). Additionally, cell culture samples were dried (40 °C) and digested for determination of trace element concentration, as detailed in Cabrita et al. (2014). Reagent blanks and international certified standards (Plankton BCR 414 and *Ulva lactuca* BCR 279, from the Community Bureau of Reference) were prepared using the same analytical procedure used for cell samples, and at the same time, to verify the accuracy of the procedure. The concentrations of Co, Ni, Cu, Zn, Cd, and Pb were determined by ICP-MS. Concentrations of the analyzed elements obtained for the reference materials were consistently within the ranges of certified values, according to the t test for a 95 % confidence level. Determination of Hg in *P. tricornutum* cells was performed by atomic absorption spectrometry with a LECO AMA254 Mercury Analyzer. Accuracy of the method was checked with the previous certified reference materials, using the same method applied for the other trace elements.

Culture samples were also taken and preserved with Lugol's solution immediately after collection, for cell counting and growth rate calculation. Cell counting was carried out on a Neubauer chamber, under a AXIOVERT 135 (Zeiss, Germany) inverted microscope, at ×400 magnification. Growth was estimated as the mean specific growth rate per day, calculated from the difference between initial and final logarithmic cell densities divided by the exposure period, as proposed by Nyholm and Källqvist (1989). Three replicates (three flasks) for each analysis were used for control and trace element-exposed cell samples.

Laser-induced fluorescence

Laser-induced fluorescence measurements of in vivo *P. tricornutum* cells were recorded with a LIF sensor based on a commercial palm-size spectrometer Ocean Optics USB4000 and a frequency-doubled Q-switched Nd: YAG laser, manufactured by Quantel (model Ultra 532 30 20HN). The laser provided up to 30-mJ pulses of 7-ns duration at the wavelength of 532 nm (second harmonic), with a pulse repetition rate up to 20 Hz. The laser spot diameter at the cell sample surface location was ~3 mm (about 1 m from the laser output aperture). Part of the fluorescence emission, reflected back to the instrument, was collected by light gathering optical train based on low cost components provided by Thorlabs, assembled within the Ø1-in lens mounting tube SM1L30. The train comprised an optical filter and a telescopic system, positioned and centered using three retaining rings SM1RR. The long pass optical filter FEL0550, with the cutoff wavelength of 550 nm and transmission of ~80 % in the region of 650–730 nm, protected the spectrometer from strong retroreflected laser light. The SMA fiber optics collimation package

F810SMA 635 was installed immediately after the filter. The SMA-connectorized fiber, commonly intended for collimating a laser beam propagating from the tip, operated in the reciprocal mode, playing a role of a principal light gathering element, which collected the fluorescence radiation over a Ø21-mm input pupil and transmitted it into an optical fiber. The fiber transported the optical signal to the spectrometer optical bench, the USB4000 f/4 asymmetrical crossed Czerny-Turner configuration with the diffraction grating Ocean Optics #9, providing nearly uniform efficiency at wavelengths from 450 to 800 nm. The spectrometer was tuned and calibrated with the help of the mercury argon calibration source CAL 2000, demonstrating the sensitivity of ~55 photons per count, and resolution of 0.19 nm per channel in the spectral range of interest (650 to 730 nm).

Data treatment and statistical analysis

Data obtained from days 2 and 4 were averaged for the 4-day study. Differences between control and trace element-exposed *P. tricornutum* cells were evaluated using Kruskal–Wallis nonparametric test. Results yielding $p < 0.05$ were considered statistically significant. All statistical analyses were performed with Statistica 6.1 Software (StatSoft, Inc.).

Results

Dissolved Co, Ni, Cu, Zn, Cd, and Pb concentrations (μg L^{-1}) at the beginning of the experiments were 2.0 ± 0.014, 2.0 ± 0.049, 3.0 ± 0.0013, 14.0 ± 0.0082, 0.055 ± 0.00057, and 0.21 ± 0.011, respectively. These results confirmed the corresponding nominal elemental concentrations of 2.0, 2.0, 3.0, 14, 0.05, and 0.2 μg L^{-1}, used for the exposure experiments in order to reproduce concentrations previously found in contaminated coastal areas. Average concentrations of trace elements within the *P. tricornutum* cells exposed to Co, Ni, Cu, Zn, Cd, Hg, Pb, and Mix, for the 4-day exposure (Fig. 1) clearly showed that element levels in exposed cells were always significantly ($p < 0.05$) higher than those found in control cells. During the exposure period, average values in exposed cells varied from 9.9 ± 3.9, 27 ± 2.3, 58 ± 6.2, 192 ± 51, 0.46 ± 0.031, 0.37 ± 0.21, and 72 ± 8.5 μg g^{-1} (d.w.), for Co, Ni, Cu, Zn, Cd, Hg, and Pb individual exposure, respectively. The cells exposed to Mix presented a similar pattern of element accumulation, with concentrations varying from 9.3 ± 1.8, 21 ± 5.3, 49 ± 4.2, 172 ± 43, 0.44 ± 0.061, 0.34 ± 0.14, and 63 ± 7.9 μg g^{-1} (d.w.), for Co, Ni, Cu, Zn, Cd, Hg, and Pb, respectively.

Average cell number and growth rate of *P. tricornutum* were similarly affected for the 4 day trace element exposure (Fig. 2). Cells growing with the presence of Co, Hg, Pb and Mix showed a significant decrease ($p < 0.05$) in biomass production, expressed both in terms of cell density and growth rate. Contrastingly, Cd induced a significant increase ($p < 0.05$) in cell density and growth rate when compared to control. The remaining trace elements had no visible effect on *P. tricornutum* biomass production.

LIF emission spectra between 650 and 790 nm for *P. tricornutum* control and trace element-exposed cells for the 4-day trace element exposure are depicted in Fig. 3. The LIF spectra showed two fluorescence emission peak maxima, located in the red (683–698 nm) and far-red (725–730 nm) regions. Control cell LIF emission spectra were kept very stable throughout the 4-day period. Emission spectra corresponding to control cells generally had higher fluorescence intensities than those of cells exposed to trace elements, particularly in the far-red region. Among all trace elements, Hg induced the highest decrease in LIF intensity in both the red and far-red regions (Fig. 3). Contrastingly, Zn appeared to induce a raise on LIF emission, mainly in the red region. Figure 4 shows maximum fluorescence (counts) deviations from control at maximum wavelength (nm) emission for all trace elements, in the red and far-red regions, for the 4-day trace element exposure. Deviations in the red area ranged from −1600 (Hg) to +1390 (Zn) counts. Larger deviations occurred in the far-red region, ranging from −10144 (Hg) to +577 (Zn) counts, more accentuated for Co, Hg, and Mix. Figure Fig. 5 shows wavelength (nm) fluorescence maxima deviations from control, for all trace elements, in the red and far-red regions, for the 4-day trace element exposure. Larger deviations occurred in the red region than in the far-red region. Detectable shifts to shorter wavelengths were associated with all trace elements, ranging from 13 nm (Hg) to 2 (Zn). The major shifts (between 8 and 13 nm) occurred for Co, Hg, and Mix. Contrastingly, wavelength shifts in the far-red region were minor, varying from −2 nm (Hg) to 0.19 (Cd).

Figure 6 shows red/far-red fluorescence ratio (F685/F735 ratio) obtained from the fluorescence spectra, of control and trace element-exposed cells, for the 4-

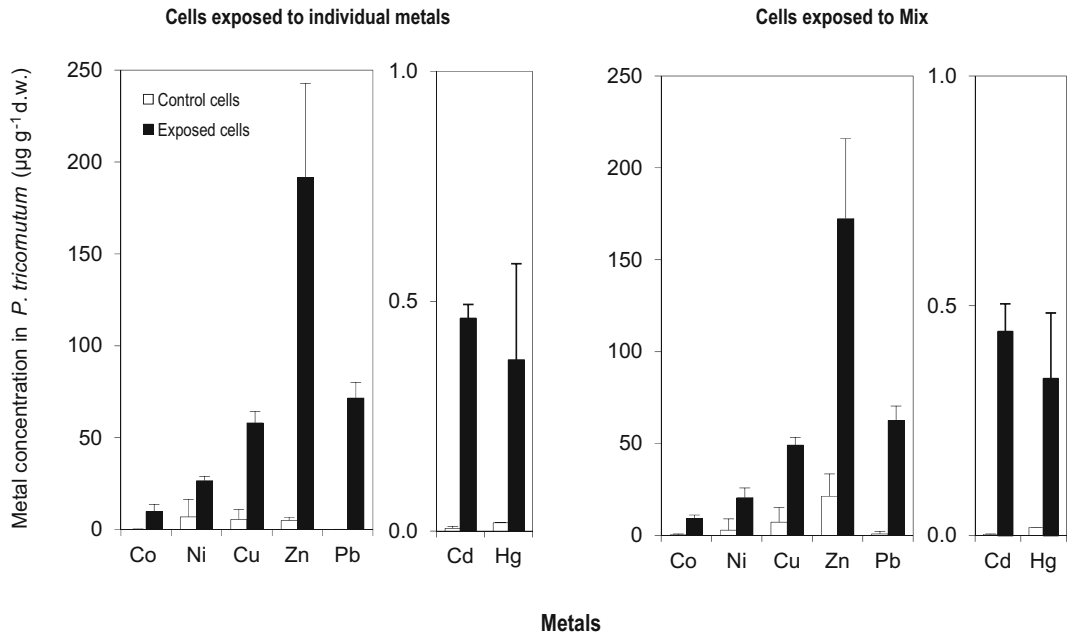

Fig. 1 Concentration of Co, Ni, Cu, Zn, Cd, Hg, and Pb (µg g^{-1} d.w.) in control (*open box*) and exposed (*shaded box*) *Phaeodactylum tricornutum* cells exposed to Co, Ni, Cu, Zn, Cd, Hg, Pb, and mixture of all trace elements combined (Mix), for the 4-day trace element exposure (mean ± standard deviation, $n = 6$). *Different letters above standard deviation bars* indicate values significantly different ($p < 0.05$) from control. Please notice the different scale for Cd and Hg

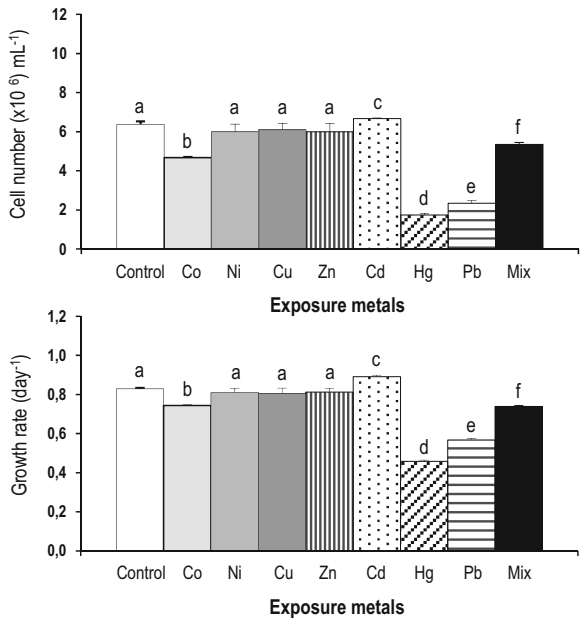

Fig. 2 Cell number (×10^6 cells L^{-1}) and growth rate (day^{-1}) of *Phaeodactylum tricornutum* in control and exposed cells to Co, Ni, Cu, Zn, Cd, Hg, Pb, and mixture of all trace elements combined (Mix), for the 4-day trace element exposure (mean ± standard deviation, $n = 6$). *Different letters above standard deviation bars* indicate values significantly different ($p < 0.05$) from control

day trace element exposure. In control cells, the F685/F735 ratio was 1.2. All trace elements, except Zn, promoted a significant increase ($p < 0.05$) on the F685/F735 ratio, in comparison with control. The ratio was highest for Co, Hg, and Mix. The large changes observed in the F685/F735 ratio were mostly due to a decrease of fluorescence intensity at 735 nm, rather than a rise at 685 nm (Fig. 4).

Figure 7 illustrates Chl *a* and carotenoid content of control and trace element-exposed cells, for the 4-day trace element exposure. Statistically significant lower concentrations ($p < 0.05$) were observed for both Chl *a* and carotenoids in cells exposed to most elements tested, except Chl *a* for Cd and carotenoids for Zn. The levels of pigments were lowest for Co, Hg, Pb, and Mix when compared to control.

Discussion

The elevated total concentrations of the determined trace elements associated with the exposed cells may explain the decrease found in the *P. tricornutum* growth rates. Trace elements variably influence microalgae growth, depending on the species due to a wide range of trace

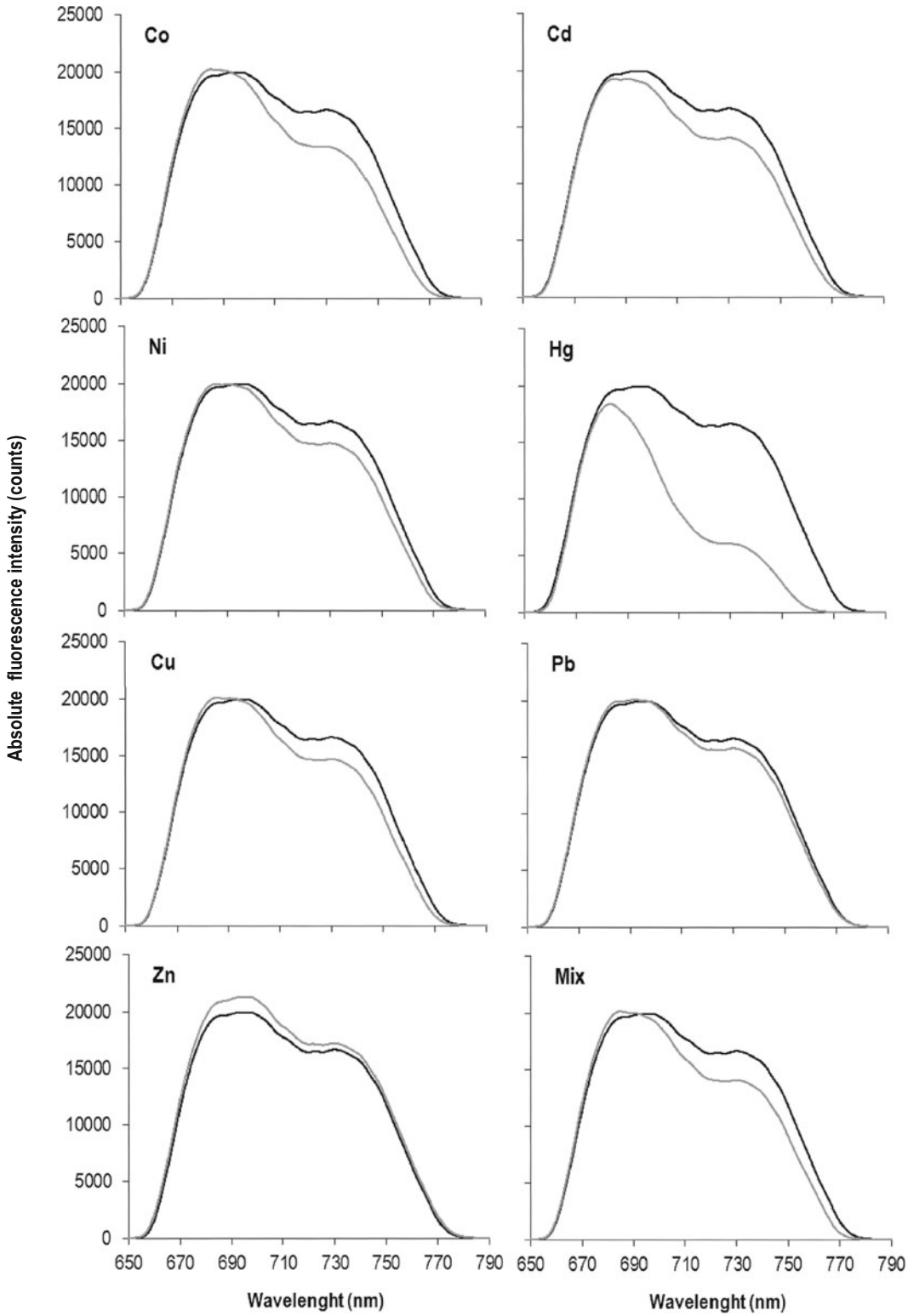

Fig. 3 Absolute fluorescence emission spectra (counts), between 650 and 790 nm, of *Phaeodactylum tricornutum* in control (*black line*) and exposed (*gray line*) cells to Co, Ni, Cu, Zn, Cd, Hg, Pb, and mixture of all trace elements combined (Mix), for the 4-day trace element exposure

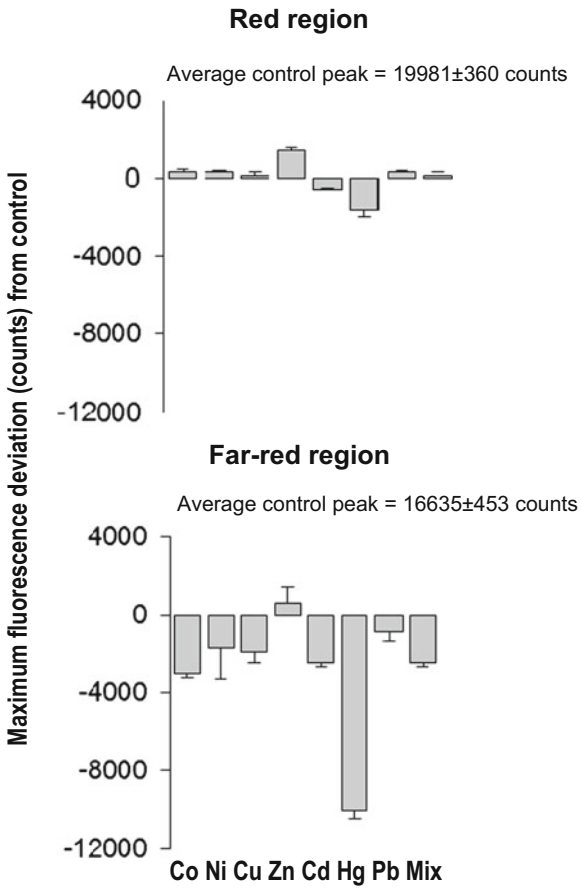

Fig. 4 Maximum fluorescence deviation (counts) from control, and average control peak value (counts), of *Phaeodactylum tricornutum* cells exposed to Co, Ni, Cu, Zn, Cd, Hg, Pb, and mixture of all trace elements combined (Mix), at the red and far-red regions, for the 4-day trace element exposure (mean ± standard deviation, $n = 6$)

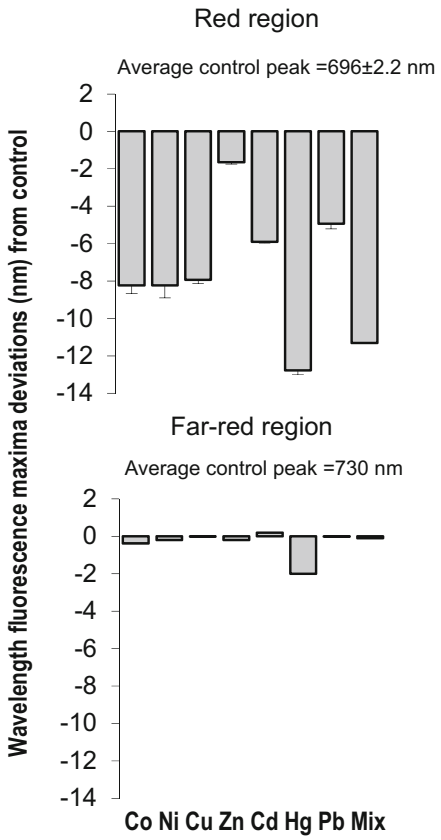

Fig. 5 Wavelength fluorescence maxima deviations (nm) from control, and average control peak value (nm), of *Phaeodactylum tricornutum* cells exposed to Co, Ni, Cu, Zn, Cd, Hg, Pb, and mixture of all trace elements combined (Mix), at the red and far-red regions, for the 4-day trace element exposure (mean ± standard deviation, $n = 6$)

element uptake and absorption efficiencies, cell compartmentalization strategies, and tolerance and detoxification mechanisms, dependent on the trace element type and concentration and cell physiological status (Sunda and Huntsman 1998). In *P. tricornutum*, trace elements have been found to suppress growth to various degrees (Markina and Aizdaicher 2006; Horvatić and Peršić 2007; Cabrita et al. 2014). Our results are in line with previous studies on the effect of trace elements on *P. tricornutum* growth, showing that Hg is the most toxic trace element causing growth inhibition, and Cd may stimulate growth, at similar trace element concentration conditions, during exponential phase (Horvatić and Peršić 2007). Although Pb and Hg do not take part in the microalgae metabolism, they have been found associated with trace element-exposed microalgae cells (Cabrita et al. 2014). Once internalized, Hg will impact several physiological processes, by binding to cytosolic ligands, allocating into organelles, and blocking functional groups of essential biomolecules (e.g., enzymes) (Le Faucheur et al. 2014), with negative repercussions to cell growth and division (Hannan and Patouillet 1972; Deng et al. 2013). Lead may also act as a serious cell toxicant even at low concentrations (Moreira et al. 2001), reducing cell growth rates (Irmer 1985), which is consistent with the observed Pb induced decrease in *P. tricornutum* cell density and growth rate.

Growth of *P. tricornutum* was only slightly affected by the total levels of Ni, Cu, and Zn associated with the exposed cells. Tolerance for Ni, Cu, and Zn, as reported for several phytoplankton species (Fisher 1981), comply with these elements being essential components in many diatom metabolic pathways (Sunda 1989). However,

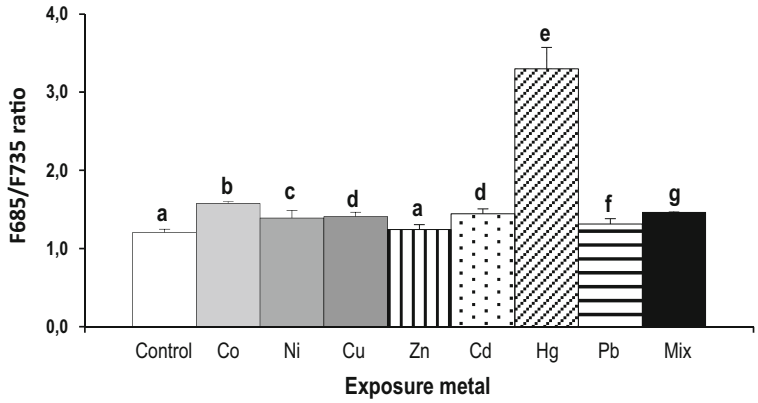

Fig. 6 Red/far red fluorescence ratio (F685/F735 ratio) of *Phaeodactylum tricornutum* in control and exposed cells to Co, Ni, Cu, Zn, Cd, Hg, Pb, and mixture of all trace elements combined (Mix), for the 4-day trace element exposure (mean ± standard deviation, $n = 6$). *Different letters above standard deviation bars* indicate values significantly different ($p < 0.05$) from control

high levels of these elements may be toxic to microalgae, as previously found for *P. tricornutum* and other microalgae under high level and chronic conditions (Sunda 1989; Horvatić and Peršić 2007), suggesting that concentrations used in this study were not sufficiently high to cause severe damage to *P. tricornutum* cells. This diatom has also been found one of the most tolerant microalgae to Cd (Torres et al. 1997) and Cu (Smith at al. 2014) toxicity. According to Scarano and Morelli (2003), *P. tricornutum* is capable to incorporate Cd-induced sulfide ions in Cd-phytochelatin complexes, producing nanometer-sized phytochelatin-coated CdS nanocrystalites which could explain the low sensitivity to Cd found for this microalgae. In addition, this species was found to maintain reduced glutathione at between 58 and 80 % of total glutathione levels over time of exposure, which would indicate low cellular stress (Smith at al. 2014).

Trace elements in excess have been found to often induce changes in cell size and morphometric parameters in microalgae, including *P. tricornutum*. Several studies have shown that changes in cell size

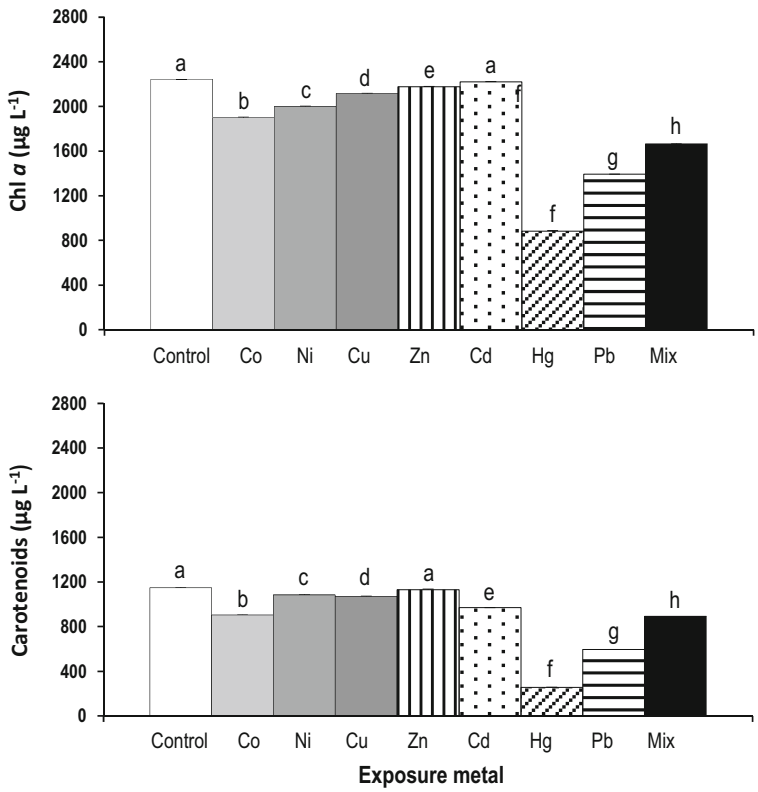

Fig. 7 Chlorophyll *a* (Chl *a*) and carotenoid concentrations (µg L^{-1}) in *Phaeodactylum tricornutum* control and cells exposed to Co, Ni, Cu, Zn, Cd, Hg, Pb, and Mix (mixture of all trace elements combined), for the 4-day trace element exposure (mean ± standard deviation, $n = 6$). *Different letters above standard deviation bars* indicate values significantly different ($p < 0.05$) from control

may vary with different trace elements and element concentrations. For instance, Cid et al. (1997) had previously found that copper concentrations of 0.5 and 1 mg L^{-1} (higher than those used in the present study) triggered an increase of cell volume of 13 and 20 % in comparison with control cells, respectively. In contrast, a study on *P. tricornutum* cell size changes in a copper-polluted environment showed that Cu concentrations two orders of magnitude higher than those used in the present study, had a negative effect on cell size (Markina and Aizdaicher 2006). Machado and Soares (2014) have found that the exposure to low trace element concentrations (Cd, Cr, Cu, and Zn) resulted in a decrease in the microalgae *Pseudokirchneriella subcapitata* cell volume whereas for higher trace element levels, an increase in the cell volume was observed. The two behaviors were found for cells of this species exposed to intermediate concentrations, depending on the element. Even though changes in cell size induced by trace elements in excess may have occurred, the highly significant increase ($p < 0.001$) in the total concentration of trace elements associated with the exposed cells comparing to control ones, indicate that the observed changes in *P. tricornutum* cell number and growth rate were likely to be a result of exposure to trace elements. These results support growth as a good indicator of the toxic action of trace elements on microalgae reflecting the cell metabolism, as was also found by Torres et al. (1997), and therefore the subsequent use of this parameter to validate the applicability of the Chl *a* fluorescence-based indicators.

The laser-induced fluorescence emission spectra of *P. tricornutum* cells showed two main emission bands in the red (683–698 nm) and the far-red (725–730 nm) regions. Comparable fluorescence emission bands have also been observed in various phytoplankton species, including *P. tricornutum* (Barbini et al. 1998), in intertidal microphytobenthos communities (Vieira et al. 2011), and in leaves of higher plants (Lichtenthaler and Rinderle 1988). Trace element effect on *P. tricornutum* indicated involvement on the photosynthesis energetic pathways. This was clearly demonstrated by the LIF emission spectra of *P. tricornutum* cells exposed to trace elements, which showed both deviations in the fluorescence emission intensity and the maximum emission wavelength in comparison to control cells. The significant decrease on fluorescence intensity in the far-red region of the spectrum observed mostly for Co, Hg, and Mix, suggests Chl *a* damage and the impairment of pigment biosynthesis pathways, which was confirmed by the lowering Chl *a* and carotenoid concentrations when compared to control cell levels. A decrease in fluorescence intensity triggered by trace elements has already been observed in higher plants and microalgae (Küpper et al. 1996; Mishra and Gopal 2005; Pandey and Gopal 2011). For instance, sublethal Cd and Hg concentrations strongly inhibit chlorophyll biosynthesis (De Filippis and Pallaghy 1976) and induce a Chl *a* decline in several microalgae species (Maurya et al. 2008). Decreased fluorescence intensity can also result from the formation of low fluorescent or nonfluorescent trace metal-substituted Chl *a* (Küpper et al. 1996). The larger deviations found in the far-red than red region suggested a decrease in reabsorption due to the decline in Chl *a*.

The large deviations in wavelength emission maxima in the red region of the fluorescence spectra in comparison to control cells, were observed for all trace elements tested, particularly for Co, Hg, and Mix (between 8 and 13 nm). These changes suggest structural changes in Chl *a* which would require confirmation using other techniques such as nuclear magnetic resonance (NMR) spectroscopy and modeling. Nevertheless, Co, Cd, Hg, and Pb, have been shown to cause structural and functional damage in photosynthesis (Aggarwal et al. 2012). Aquatic grass plants and microalgae submitted to trace element stress, have been shown wavelength decrease due to substitution of magnesium (Mg) in the Chl *a* molecule by Ni, Cu, Zn, Cd, Hg, and Pb that caused a decline in the net photosynthesis (Küpper et al. 1996, 2002). Incorporation of divalent trace elements in Chl *a* prevents photosynthetic light-harvesting in the affected antenna pigments and consequently restrains electron transfer in the reaction centers, leading to photosynthesis collapse (Watanabe et al. 1985; Küpper et al. 1996). The observed much larger wavelength deviations allocated in the red as compared to the far-red region may imply that PSII chlorophylls were more affected by trace elements than the PSI chlorophylls. Slight or even undetected in vivo inhibition of PSI and complete inhibition of PSII have been reported for several plant species, including phytoplankton (Küpper et al. 2002). If Mg substitution occurred during the present experiments, this would probably have been a consequence of the relatively low environmental water trace element concentrations (<0.2 μmol L^{-1}) used in this study, as only PSII chlorophylls have been shown to be accessible to trace element ions at low levels (<0.5 μmol L^{-1}),

whereas under high concentrations (>50 μmol L^{-1}) Mg substitution occurs in all chlorophylls (Küpper et al. 1996). These results point to deviation in wavelength emission maxima as adequate and reliable indicator for the detection of trace element stress.

The fluorescence signal deviations were clearly reflected on the F685/F735 ratios found for the tested elements, except Zn. The significant increase in the ratio, more accentuated for Co, Hg, and Mix, compared to control cell ratio, was mostly due to a decline in fluorescence intensity at 735 nm, rather than to a rise in fluorescence at 685 nm. This suggests that total trace elements associated with the cells not only induced alterations in the PSII efficiency but also affect the distribution of excitation energy between the two photosystems (state transitions) (Wollman 2001). The rise in red/far-red ratios in response to trace element toxicity is comparable to different types of stress inflicted on many plant species showing breakdown or reduced synthesis of Chl *a* and damage in the photosynthetic apparatus, caused by nutrient stress (Subhash and Mohanan 1997), Cd exposure (Maurya and Gopal 2008), herbicides, and senescence processes (D'Ambrosio et al. 1992). These results point to the use of the F685/F735 ratio as an adequate indicator for the detection of trace element stress which is in line with several studies demonstrating that this ratio can be used to assess relative Chl *a* concentrations and photosynthetic efficiency (Lichtenthaler et al. 1996), stress events, and stress tolerance in many plant species (D'Ambrosio et al. 1992; Buschmann 2007).

Conclusions

This study clearly shows F685/F735 ratio and deviation in wavelength emission maxima to be reliable and suitable Chl *a* fluorescence-based indicators for trace element stress detection and monitoring in marine systems, using *P. tricornutum* as biomonitor tool. These indicators discriminated the toxic action of trace elements, highlighting Co and Hg as the most affecting elements to this species. Growth and pigment changes supported their applicability as indicators. The LIF-based techniques have potential to effectively and reliably assess trace element impacts on phytoplankton communities, during events of element mobilization, such as dredging, harbor or industrial trace element contaminated waste disposal activities, highlighting their applicability for remote sensing and trace element contamination screening in marine coastal areas. Finally, *P. tricornutum* is a promising model species and biomonitor tool with applications for trace element contamination assessment in marine ecosystems.

Acknowledgments M.T. Cabrita express appreciation for the support from the "Fundação para a Ciência e a Tecnologia" (FCT), through Grant No. SFRH/BPD/50348/2009. C. Gameiro and this work were also funded by the Fundação para a Ciência e a Tecnologia (FCT, Portugal) within the framework of the project BenthicLIF-Estuarine phytobenthic communities studied by laser induced fluorescence (PTDC/MAR/117929/2010). The authors would like to thank the anonymous reviewers for their constructive comments, which helped improve the manuscript.

References

Aggarwal, A., Sharma, I., Tripathi, B.N., Munjal, A.K., Baunthiyal, M., & Sharma, V. (2012). Metal toxicity and Photosynthesis. In S. Itoh, P. Mohanty, K.N. Guruprasad (Eds.), *Photosynthesis: overviews on recent progress and future perspectives* (pp. 229–236), Chapter 6.

Apostol, S., Viau, A. A., Tremblay, N., Briantais, J.-M., Prasher, S., Parent, L.-E., & Moya, I. (2003). Laser-induced fluorescence signatures as a tool for remote monitoring of water and nitrogen stresses in plants. *Canadian Journal of Remote Sensing, 29*(1), 57–65.

Baker, N. R. (2008). Chlorophyll fluorescence: a probe of photosynthesis *in vivo*. *Annual Review of Plant Biology, 59*, 89–113.

Barbini, R., Colao, F., Fantoni, R., Micheli, C., Palucci, A., & Ribezzo, S. (1998). Design and application of a lidar fluorosensor system for remote monitoring of phytoplankton. *ICES Journal of Marine Science, 55*, 793–802.

Brand, L. E., Sunda, W. G., & Guillard, R. R. L. (1986). Reduction of marine phytoplankton reproduction rates by copper and cadmium. *Journal of Experimental Marine Biology and Ecology, 96*, 225–250.

Buschmann, C. (2007). Variability and application of the chlorophyll fluorescence emission ratio red/far-red of leaves. *Photosynthesis Research, 92*, 261–271.

Cabrita, M. T., Raimundo, J., Pereira, P., & Vale, C. (2014). Immobilised *Phaeodactylum tricornutum* as biomonitor of trace element availability in the water column during dredging. *Environmental Science and Pollution Research, 21*(5), 3572–2581.

Cid, A., Herrero, C., Torres, E., & Abalde, J. (1995). Copper toxicity on the marine microalga *Phaeodactylum tricornutum*: effects on photosynthesis and related parameters. *Aquatic Toxicology, 31*, 165–174.

Cid, A., Torres, E., Herrero, C., & Abalde, J. E. (1997). Disorders provoked by copper in the marine diatom Phaeodactylum tricornutum in short-time exposure assays. *Cahiers de Biologie Marine, 38*, 201–206.

Cotté-Krieff, M.-H., Guieu, C., Thomas, A. J., & Martin, J.-M. (2000). Sources of Cd, Cu, Ni and Zn in Portuguese coastal waters. *Marine Chemistry, 71*, 199–214.

D'Ambrosio, N., Szábo, K., & Lichtenthaler, H. K. (1992). Increase of the chlorophyll fluorescence ratio F690/F735 during the autumnal chlorophyll breakdown. *Radiation and Environmental Biophysics, 31*, 51–62.

Dahn, H. G., Günther, K. P., & Lüdeker, W. (1992). Characterization of drought stress of maize and wheat canopies by means of resolved laser induced fluorescence. *EARSel Advances in Remote Sensing, 1*(2-II), 12–19.

Davison, W., & Zhang, H. (1994). *In situ* speciation measurements of trace components in natural waters using thin-film gels. *Nature, 367*, 546–548.

De Filippis, L. F., & Pallaghy, C. K. (1976). The effect a sublethal concentration of mercury and zinc on *Chlorella*. I. Growth characteristic and uptake of metals. *Zeitschrift für Pflanzenphysiologie, 78*, 197–207.

De Filippis, L. F., & Pallaghy, C. K. (1994). Heavy metals: sources and biological effects. In L. C. Rai & J. P. Gaur (Eds.), *Advances in limnology series: algae and water pollution* (pp. 31–77). Stuttgart: E. Scheizerbartsche Press.

Deng, C. N., Zhang, D. Y., Pan, X. L., Chang, F. Q., & Wang, S. Z. (2013). Toxic effects of mercury on PSI and PSII activities, membrane potential and transthylakoid proton gradient in Microsorium pteropus. *Journal of Photochemistry and Photobiology B: Biology, 127*(5), 1–7.

Doney, S. C. (2010). The growing human footprint on coastal and open-ocean biogeochemistry. *Science, 328*, 1512–1516.

Eggleton, J., & Thomas, K. V. (2004). A review of factors affecting the release and bioavailability of contaminants during sediment disturbance events. *Environment International, 30*, 973–980.

Fisher, N. S. (1981). On the selection for heavy metal tolerance in diatoms from the Derwent Estuary, Tasmania. *Australian Journal of Marine and Freshwater Research, 32*, 555–561.

Franck, F., Juneau, P., & Popovic, R. (2002). Resolution of the photosystem I and photosystem II contributions to chlorophyll fluorescence of intact leaves at room temperature. *Biochimica et Biophysica Acta, 1556*, 239–246.

González-Dávila, M. (1995). The role of phytoplankton cells on the control of heavy metal concentration in seawater. *Marine Chemistry, 48*(3–4), 215–236.

Govindjee. (1995). Sixty-three years since Kautsky: chlorophyll *a* fluorescence. *Australian Journal of Plant Physiology, 22*, 131–160.

Guillard, R. R. L., & Ryther, J. H. (1962). Studies on marine planktonic diatoms, I. Cyclotella nana Hustedt and Detonula confervaceae (Cleve) Gran. *Canadian Journal of Microbiology, 8*(2), 229–239.

Hannan, P. J., & Patouillet, C. (1972). Effect of mercury on algal growth rates. *Biotechnology and Bioengineering, 14*, 93–101.

Horvatić, J., & Peršić, V. (2007). The Effect of Ni^{2+}, Co^{2+}, Zn^{2+}, Cd^{2+} and Hg^{2+} on the growth rate of marine diatom *Phaeodactylum tricornutum* Bohlin: microplate growth inhibition test. *Bulletin of Environmental Contamination and Toxicology, 79*, 494–498.

Irmer, G. (1985). Zum einfluß der apparatefunktion auf die bestimmung von streuquerschnitten und lebensdauern aus optischen phononenspektren. *Experimentelle Technik der Physik, 33*, 501–506.

Jakimska, A., Konieczka, P., Skóra, K., & Namieśnik, J. (2011). Bioaccumulation of metals in tissues of marine animals, Part I: the role and impact of heavy metals on organisms. *Polish Journal of Environmental Studies, 20*(5), 1117–1125.

Kumar, K. S., Dahms, H.-U., Lee, J.-S., Kim, H. C., Lee, W. C., & Shin, K.-H. (2014). Algal photosynthetic responses to toxic metals and herbicides assessed by chlorophyll a fluorescence. *Ecotoxicology and Environmental Safety, 104*, 51–71.

Küpper, H., Küpper, F., & Spiller, M. (1996). Environmental relevance of heavy metal substituted chlorophylls using the example of water plants. *Journal of Experimental Botany, 47*(295), 259–266.

Küpper, H., Setlik, I., Spiller, M., Küpper, F. C., & Prasil, O. (2002). Heavy-metal-induced inhibition of photosynthesis: targets of in vivo heavy metal chlorophyll formation. *Journal of Phycology, 38*, 429–441.

Lavrov, A., Utkin, A. B., Marques da Silva, J., Vilar, R., Santos, N. M., & Alves, B. (2012). Water stress assessment of cork oak leaves and maritime pine needles bases on LIF spectra. *Optics and Spectroscopy, 112*, 271–279.

Le Faucheur, S., Campbell, P. G. C., Fortin, C., & Slaveykova, V. (2014). Interactions between mercury and phytoplankton: speciation, bioavailability, and internal handling. *Environmental Toxicology and Chemistry, 33*(6), 1211–1224.

Lichtenthaler, H. K., & Rinderle, U. (1988). The role of chlorophyll fluorescence in the detection of stress conditions in plants. *CRC Critical Reviews in Analytical Chemistry, 19*, S29–S85.

Lichtenthaler, H. K., Lang, M., Sowinska, M., Heisel, F., & Miehé, J. A. (1996). Detection of vegetation stress via a new high resolution fluorescence imaging system. *Journal of Plant Physiology, 148*(5), 599–612.

Machado, M. D., & Soares, E. V. (2014). Modification of cell volume and proliferative capacity of Pseudokirchneriella subcapitata cells exposed to metal stress. *Aquatic Toxicology, 147*, 1–6.

Markina, Z. V., & Aizdaicher, N. A. (2006). Content of photosynthetic pigments, growth, and cell size of microalgae *Phaeodactylum tricornutum* in the copper-polluted environment. *Russian Journal of Plant Physiology, 53*(3), 305–309.

Maurya, R., & Gopal, R. (2008). Laser-induced fluorescence ratios of Cajanus cajan L. Under the stress of cadmium and its correlation with pigment content and pigment ratios. *Applied Spectroscopy, 62*(4), 433–438.

Maurya, R., Prasad, S. M., & Gopal, R. (2008). LIF technique offers the potential for the detection of cadmium-induced alteration in photosynthetic activities of *Zea mays* L. *Journal of Photochemistry and Photobiology C Photochemistry Reviews, 9*, 29–35.

Mishra, K. B., & Gopal, R. (2005). Laser induced fluorescence spectra of leaves of wheat seedlings growing under cadmium stress. *General and Applied Plant Physiology, 31*, 181–196.

Moreira, E. G., Vassilieff, I., & Vassilieff, V. S. (2001). Developmental lead exposure. Behavioral alterations in the short and long term. *Neurotoxicology and Teratology, 23*, 489–495.

Nyholm, N., & Källqvist, T. (1989). Methods for growth inhibition toxicity tests with freshwater algae. *Environmental Toxicology and Chemistry, 8*(8), 689–703.

OECD, Organisation for Economic Co-operation and Development, Freshwater algal and cyanobacteria, growth

inhibition test - test guideline 201 (2002). OECD Guidelines for the testing of chemicals, Paris, France, 1(2), 1–25.

Pan, K., & Wang, W.-X. (2012). Trace metal contamination in estuarine and coastal environments in China. *Science of the Total Environment, 421–422*, 3–16.

Pandey, J. K., & Gopal, R. (2011). Laser-induced chlorophyll fluorescence and reflectance spectroscopy of cadmium treated *Triticum aestivum* L. Plants. *Spectroscopy: An International Journal, 26*(2), 129–139.

Pfündel, E. (1998). Estimating the contribution of photosystem I to total leaf chlorophyll fluorescence. *Photosynthesis Research, 56*, 185–195E.

Reed, R. H., & Gadd, G. M. (1989). Metal tolerance in eukaryotic and prokaryotic algae. In A. J. Shaw (Ed.), *Heavy metal tolerance in plants: evolutionary aspects* (pp. 105–118). Boca Raton: CRC Press.

Rogers, S. I., & Greenaway, B. A. (2005). UK perspective on the development of marine ecosystem indicators. *Marine Pollution Bulletin, 50*, 9–19.

Scarano, G., & Morelli, E. (2003). Properties of phytochelatin-coated CdS nanocrystallites formed in a marine phytoplanktonic alga (*Phaeodactylum tricornutum*, Bohlin) in response to Cd. *Plant Science, 165*, 803–810.

Schuerger, A. C., Capelle, G. A., Di Benedetto, J. A., Mao, C., Chi, N., Mark, T., Evans, D., Richards, J. T., Blank, T. A., & Stryjewski, E. C. (2003). Comparison of two hyperspectral imaging and two laser-induced fluorescence instruments for the detection of zinc stress and chlorophyll concentration in bahia grass (*Paspalum notatum* Flugge.). *Remote Sensing of Environment, 84*, 572–588.

Smith, C. L., Steele, J. E., Stauber, J. L., Dianne, F., & Jolley, D. F. (2014). Copper-induced changes in intracellular thiols in two marine diatoms: *Phaeodactylum tricornutum* and *Ceratoneis closterium. Aquatic Toxicology, 156*, 211–220.

Strickland, J. D. H., & Parsons, T. R. (1968). A practical handbook of seawater analysis. *Ottawa: Fisheries Research Board of Canada Bulletin, 167*. 311 pp.

Subhash, N., & Mohanan, C. N. (1997). Curve fit analysis of chlorophyll fluorescence spectra: application to nutrient stress detection in sunflower. *Remote Sensing of Environment, 60*, 347–356.

Sunda, W. G. (1989). Trace metal interactions with marine phytoplankton. *Biological Oceanography, 6*(5–6), 411–442.

Sunda, W. G., & Huntsman, S. A. (1998). Processes regulating cellular metal accumulation and physiological effects: phytoplankton as model systems. *Science of the Total Environment, 219*(2–3), 165–181.

Thomas, W. H., Hollibaugh, J. T., Seibert, D. L. R., & Wallace, G. T., Jr. (1980). Toxicity of a mixture of ten metals to phytoplankton. *Marine Ecology Progress Series, 2*, 213–220.

Torres, E., Cid, A., Fidalgo, P., Herrero, C., & Abalde, J. (1997). Long-chain class III metallothioneins as a mechanism of cadmium tolerance in the marine diatom *Phaeodactylum tricornutum* Bohlin. *Aquatic Toxicology, 39*, 231–246.

Tortell, P. D., & Price, N. M. (1996). Cadmium toxicity and zinc limitation in centric diatoms of the genus *Thalassiosira. Marine Ecology Progress Series, 138*, 245–254.

Vieira, S., Utkin, A. B., Lavrov, A., Santos, N. M., Vilar, R., Marques da Silva, J., & Cartaxana, P. (2011). Effects of intertidal microphytobenthos migration on biomass determination via laser-induced fluorescence. *Marine Ecology Progress Series, 432*, 45–52.

Watanabe, T., Machida, K., Suzuki, H., Kobayashi, M., & Honda, K. (1985). Photoelectrochemistry of metallochlorophylls. *Coordination Chemistry Reviews, 64*, 207–224.

Wollman, F. A. (2001). State transitions reveal the dynamics and flexibility of the photosynthetic apparatus. *EMBO Journal, 20*(14), 3623–3630.

Zhang, H., & Davison, W. (1995). Performance characteristics of diffusion gradients in thin-film for the in situ measurement of trace-metalin aqueous solution. *Analytical Chemistry, 67*, 3391–3400.

Zhang, H., & Davison, W. (1999). Diffusional characteristics of hydrogels used in DGT and DET techniques. *Analytica Chimica Acta, 398*, 329–340.